

Supporting Information

Molecular Reconfigurations Enabling Active Liquid-Solid Interfaces for Ultrafast Li Diffusion Kinetics in 3D Framework of Garnet Solid State Electrolyte

Fuxin Wei, Shufen Wu, Jiliang Zhang, Hongyang Fan, Liuyang Wang, Vincent Wing-hei Lau, Sizhou Hou, Minmin Zhang, Jiafeng Zhang*, Bo Liang*, Ruirui Zhao*

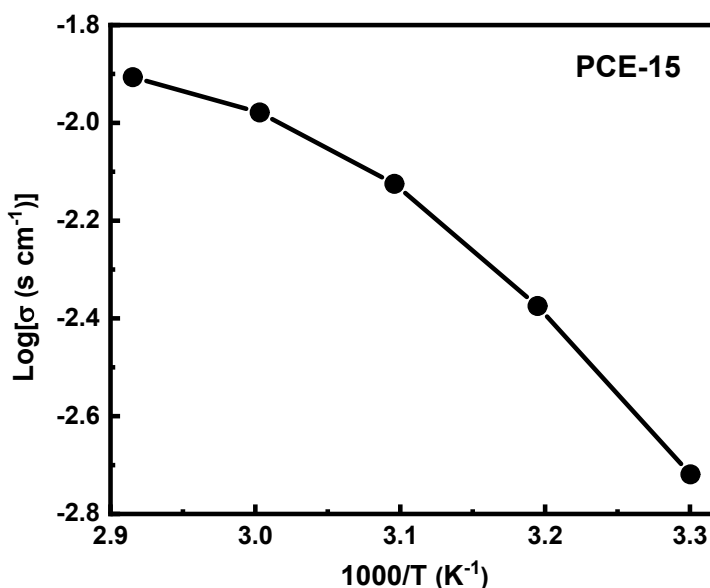


Figure S1. Arrhenius plot of PCE-15 conductivity.

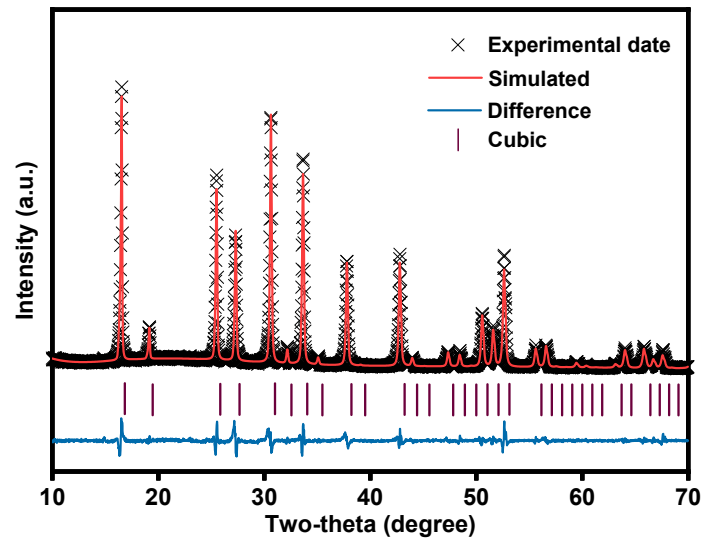


Figure S2. The XRD pattern and Rietveld refinement result for LLZO.

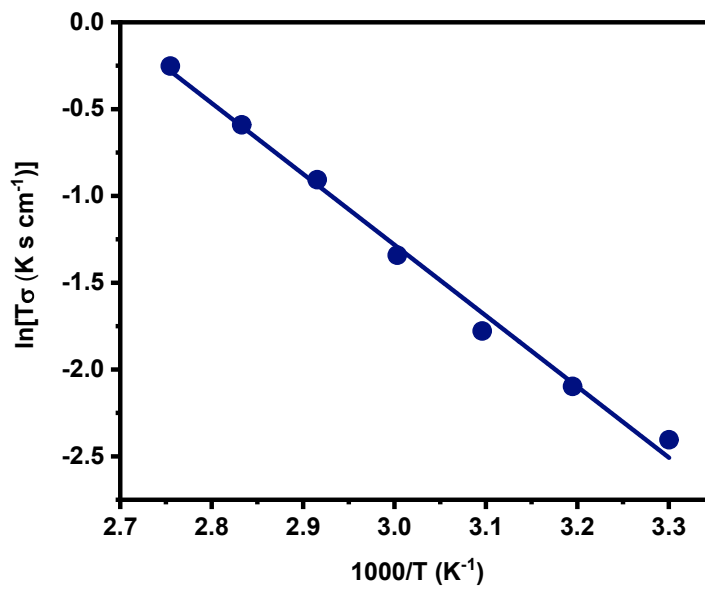


Figure S3. Arrhenius plot of LLZO conductivity.

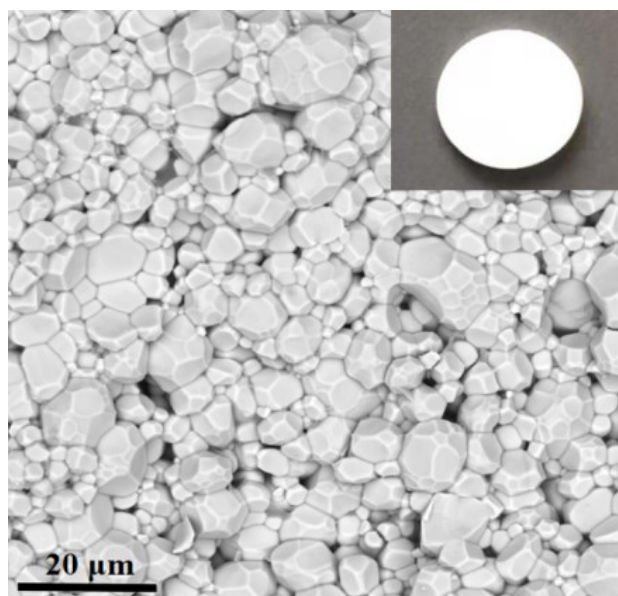


Figure S4. Cross-sectional SEM image of LLZO. The inset shows an optical image of the LLZO pellet.

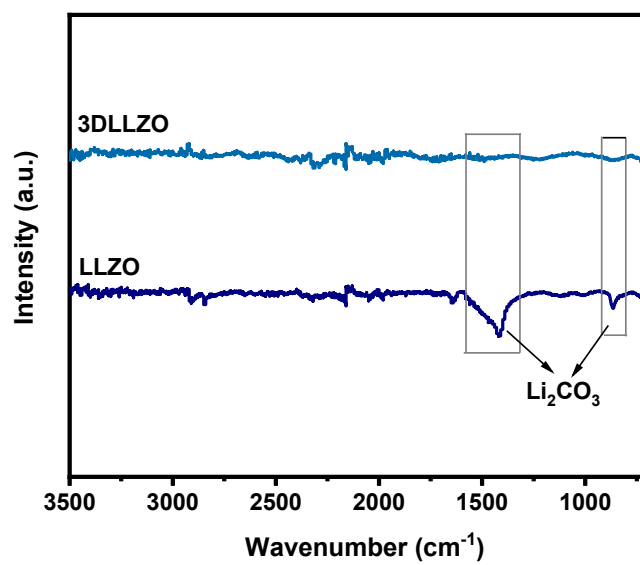


Figure S5. FTIR spectra of 3DLLZO and LLZO.

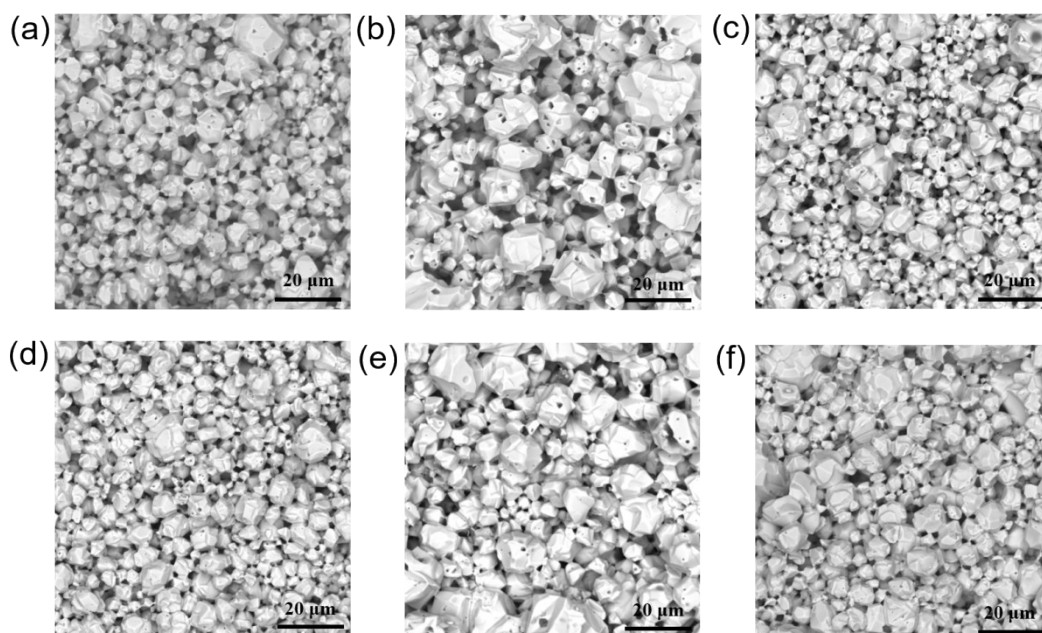


Figure S6. Surface SEM image of LLZO treated with HNO₃ at a) 2.5 min, b) 5min, c) 7.5 min, d) 10 min, e) 15 min and f) 20 min.

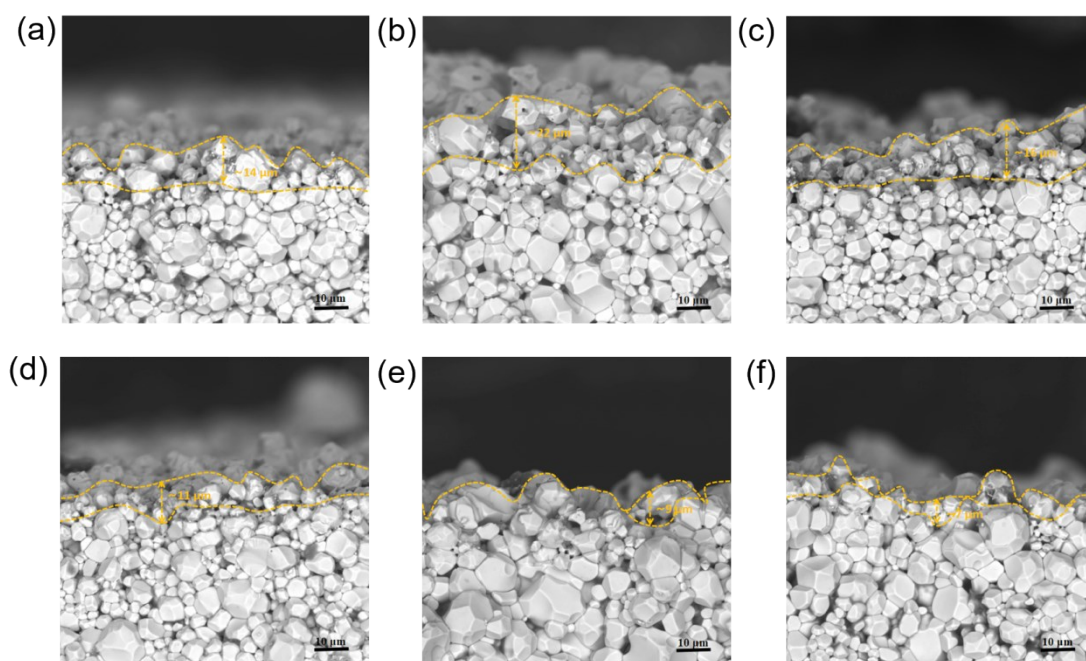


Figure S7. Cross-sectional SEM image of LLZO treated with HNO₃ at a) 2.5 min, b) 5min, c) 7.5 min, d) 10 min, e) 15 min and f) 20 min.

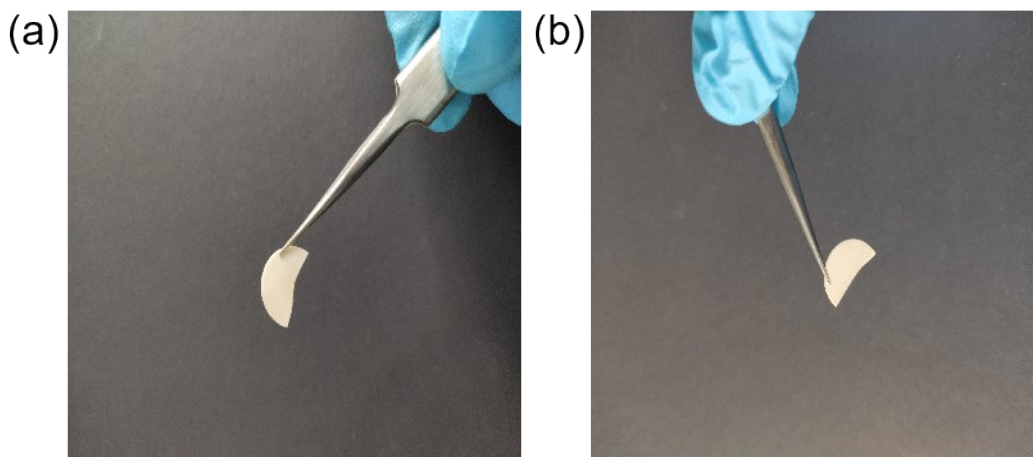


Figure S8. The optical image of LLZO a) before and b) after soaking in SN for ten days.

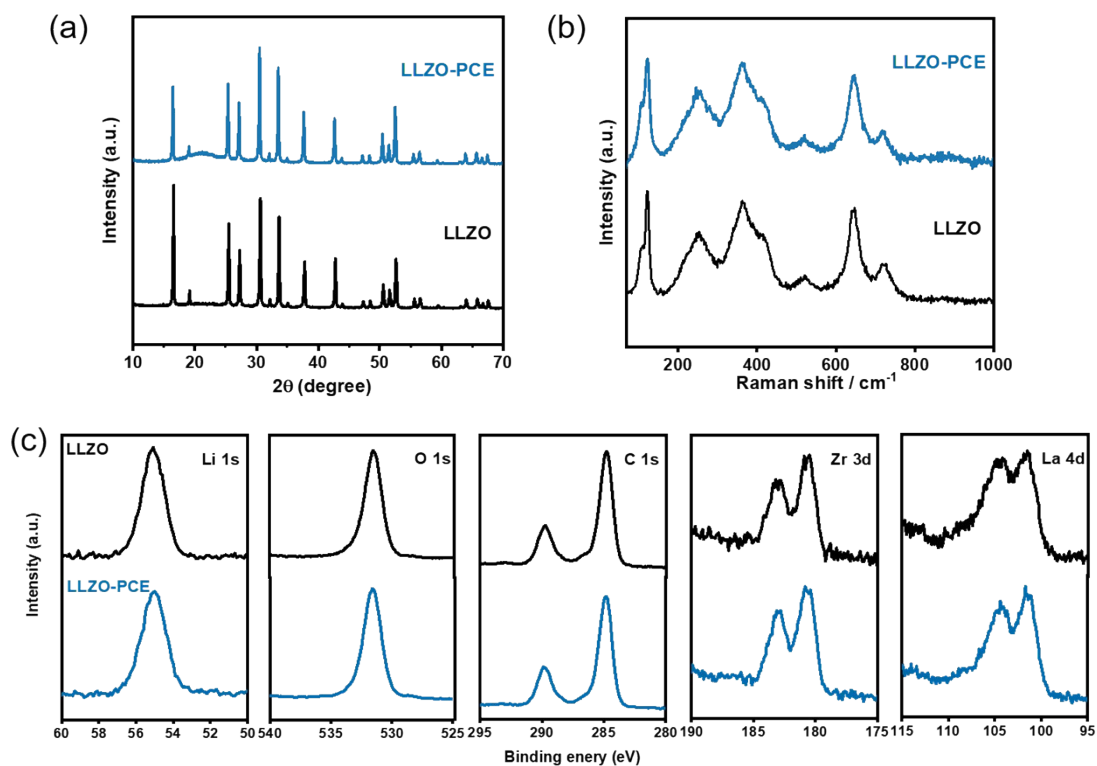


Figure S9. a) X-ray diffraction patterns, b) Raman spectra and c) XP spectra of LLZO before and after immersion in PCE for ten days.

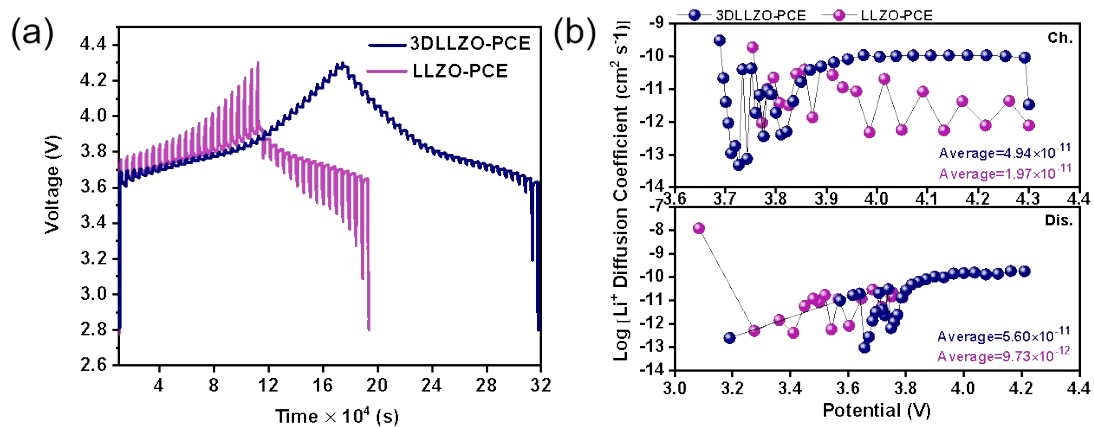


Figure S10. a) The charge and discharge GITT curves and b) the Li^+ diffusion coefficients at different voltages of NCM/3DLLZO-PCE/Li and NCM/LLZO-PCE/Li.

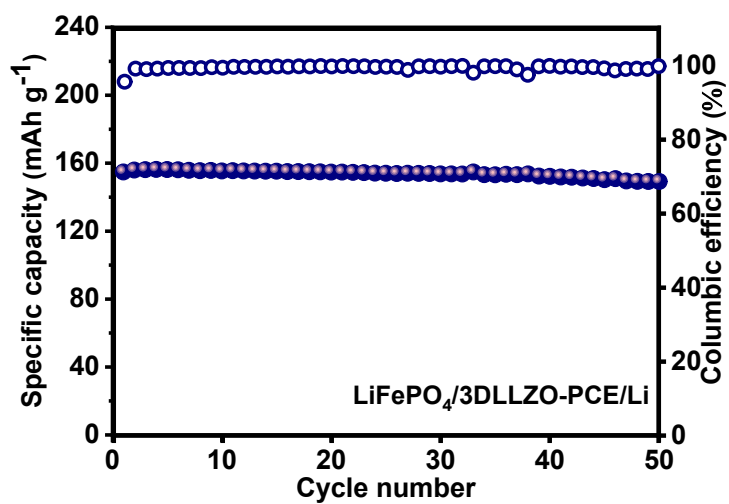


Figure S11. Cycling performance of LiFePO₄/3DLLZO-PCE/Li cell.

Figure S12. Equivalent circuits for different cells characterized in Figure 5.

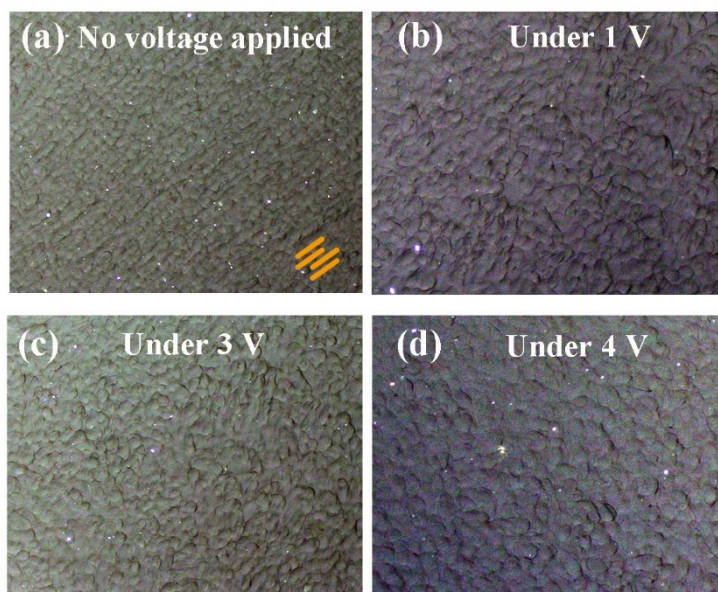


Figure S13. The optical microscopy images of the PCE under different potentials. The morphological change of plastic crystals is generally related to the molecular reorganization [1].

Table S1. The values of I_0 , I_{ss} , R_0 , R_{ss} , and the calculated values of t_{Li^+} at RT.

electrolytes	$I_0/\mu\text{A}$	$I_{ss}/\mu\text{A}$	R_0/Ω	R_{ss}/Ω	$\Delta V/\text{mV}$	t_{Li^+}
3DLLZO-PCE	11.40	8.54	691	883	10	0.65
LLZO-PCE	11.30	6.97	810	1130	10	0.25

Table S2. Performance comparison of solid state batteries with NCM as cathode material using different modification strategies.

Cathode composite	Solid electrolyte	Specific parameters	test Strategy	Discharge capacity (mAh g ⁻¹)	Capacity retention after Ref. cycling(%)	Ref.
Li(Ni _{0.5} Mn _{0.3} Co _{0.2})O ₂	Li ₁₀ GeP ₂ S ₁₂	RT 0.1C 1.9–3.8V	An interfacial layer of LiNbTaO ₃	156.4(1st) 94.5(150th)	60	2
LiNi _{0.33} Mn _{0.33} Co _{0.33} O ₂	Li _{6.28} La ₃ Zr ₂ Al _{0.24} O ₁₂	100°C cm ⁻² 2.0–4.5 V	10 mA A Li ₂ SiO ₃ interlayer	138(1st) ≈110(10th)	3	4
LiNi _{0.6} Mn _{0.2} Co _{0.2} O ₂	Li _{6.4} La ₃ Zr _{1.4} Ta _{0.6} O ₁₂	RT 0.05C 3.0–4.2V	Li ₃ BO ₃ as sintering aid and buffer layer	106(1st)	—	4
LiNi _{0.5} Co _{0.2} Mn _{0.3} O ₂	Li _{6.5} La ₃ Zr _{1.5} Ta _{0.5} O ₁₂	25°C	0.2C 10 μL of EC/DMC electrolyte wetting at the interface	≈142(1st) ≈115(150th)	81	5
LiNi _{0.5} Co _{0.2} Mn _{0.3} O ₂	Li _{6.75} La ₃ Zr _{1.75} Ta _{0.25} O ₁₂	80 °C, 5 μA·cm ⁻² 3.0–4.6 V	In-situ spinel Li[Ti _{0.1} Mn _{0.9}] ₂ O ₄ formed at the surface after annealing	123.3 (1st) 76.6 (5th)	62	6
LiNi _{0.5} Co _{0.2} Mn _{0.3} O ₂	Li _{6.35} Ga _{0.15} La ₃ Zr _{1.8} Nb _{0.2} O ₁₂	RT 0.1C 2.8–4.3V	Interface layer of 3D LLZO frame combined with plastic crystal electrolyte	165.3 (1st) 156.4 (100th)	95	This work

Table S3. Literature overview of the strategies to overcome the interfacial resistance of $R_{\text{cathode/SE}}$ and comparison with the current work.

Electrolyte	Test temperature (°C)	Strategy	The interfacial resistance of $R_{\text{cathode/SE}}$ ($\Omega \text{ cm}^2$)	Ref.
$\text{Li}_{6.4}\text{La}_3\text{Zr}_{1.4}\text{Ta}_{0.6}\text{O}_{12}$	RT	A plastic crystal interlayer based on succinonitrile with a fluoroethylene carbonate additive	400	25
$\text{Li}_{6.5}\text{La}_{2.5}\text{Ba}_{0.5}\text{ZrNbO}_{12}$	25	Employing ionic liquid electrolyte (ILE) thin interlayers at the electrodes/electrolyte interface	265	45
$\text{Li}_7\text{La}_{2.75}\text{Ca}_{0.25}\text{Zr}_{1.75}\text{Nb}_{0.25}\text{O}_{12}$	RT	Gel electrolyte was used as an interlayer	248	46
$\text{Li}_{6.75}\text{La}_3\text{Zr}_{1.75}\text{Nb}_{0.25}\text{O}_{12}$	25	LiCoO_2 was deposited by pulsed-laser deposition (PLD)	170	47
$\text{Li}_7\text{La}_3\text{Zr}_2\text{O}_{12}$	—	Deposition of a Nb metal layer onto $\text{Li}_7\text{La}_3\text{Zr}_2\text{O}_{12}$	150	48
$\text{Li}_{6.35}\text{Ga}_{0.15}\text{La}_3\text{Zr}_{1.8}\text{Nb}_{0.2}\text{O}_{12}$	RT	A plastic crystal interlayer based on succinonitrile with LiTFSI	278	This work
		Interface layer of 3D LLZO frame combined with plastic crystal electrolyte	54	

References

- [1]. A. Luzio, L. Criante, V. D'Innocenzo, M. Caironi, Sci Rep. 2013, 3, 3425.
- [2]. C H Wang, R Z Yu, S Hwang, J W Liang, X N Li, C T Zhao, Y P Sun, J W Wang, N Holmes, R Y Li, H Huang, S Q Zhao, L Zhang, S G Lu, D Su, X L Sun. Energy Storage Mater., 2020, 30, 98-103.
- [3]. G V Alexander, N C Rosero-Navarro, A Miura, K Tadanaga, R Murugan. J. Mater. Chem. A, 2018, 6, 21018.
- [4]. D W Wang, Q Sun, J Luo, J N Liang, Y P Sun, R Y Li, K Adair, L Zhang, R Yang, S G Lu, H Huang, X L Sun. ACS Appl. Mater. Interfaces, 2019, 11, 4954–4961.
- [5]. M L Cai, Y Lu, J M Su, Y D Ruan, C H Chen, B V R Chowdari, Z Y Wen. ACS Appl. Mater. Interfaces, 2019, 11, 35030-35038.
- [6]. T Liu, Y B Zhang, X Zhang, L Wang, S X Zhao, Y H Lin, Y Shen, J Luo, L L Li, C W Nan. J. Mater. Chem. A, 2018,6, 4649-4657.